Materials LAB 2022, 1, 220046

Supporting Information

Tin Sulfide Chalcogel derived SnS_x for CO_2 Electroreduction

Published as part of the Virtual Special Issue "Mercouri G. Kanatzidis at 65"

Jingwen Bai[1,2]†, Lijun Yang[2]†, Yuanyuan Zhang[1,2], Xiaofu Sun[3], Jian Liu[1,2]*

[1]College of Materials Science and Engineering, Qingdao University of Science and Technology, Qingdao 266042, P.R. China
[2]Qingdao Institute of Bioenergy and Bioprocess Technology, Chinese Academy of Sciences, Shandong Energy Institute, Qingdao 266101, P.R. China
[3]Beijing National Laboratory for Molecular Sciences, CAS Key Laboratory of Colloid and Interface and Thermodynamics, CAS Research/Education Center for Excellence in Molecular Sciences, Institute of Chemistry, Chinese Academy of Sciences, Beijing 100190, P.R. China
† These authors contributed equally to this work.
*Corresponding Authors, E-mail: liujian@qibebt.ac.cn

Keywords: Chalcogel; Carbon dioxide; electrocatalysis; Tin sulfide; CV activation

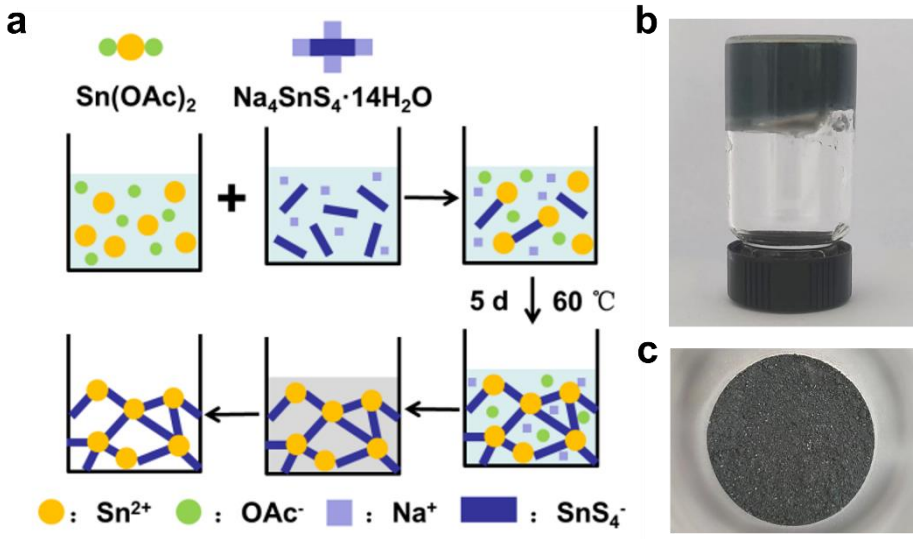

Figure S1. (a) Synthesis scheme of tin sulfide chalcogel SnS_x. The photographs of (b) tin sulfide chalcogel SnS_x and (c) SnS_x powders obtained after freeze-drying.

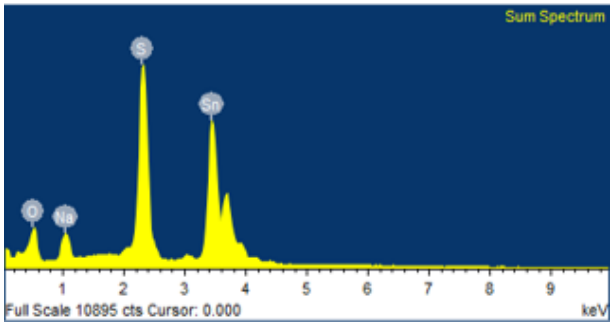

Figure S2. The EDS spectra of the SnS_x powders.

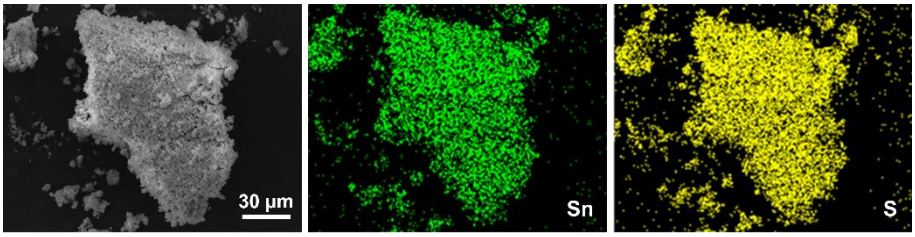

Figure S3. EDS elemental mapping of the SnS_x powders.

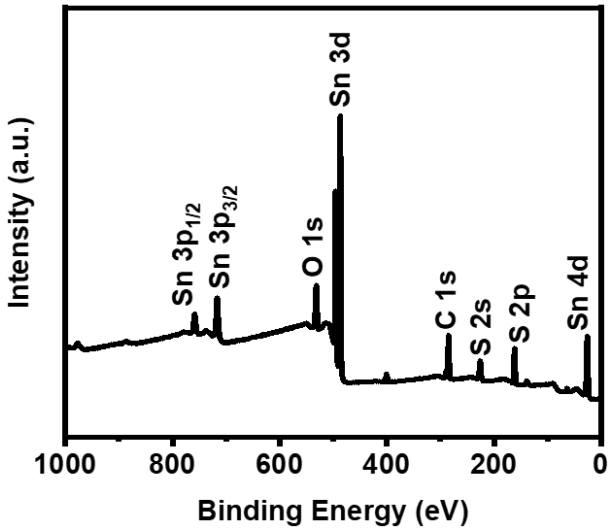

Figure S4. XPS survey spectra of the SnS_x powders.

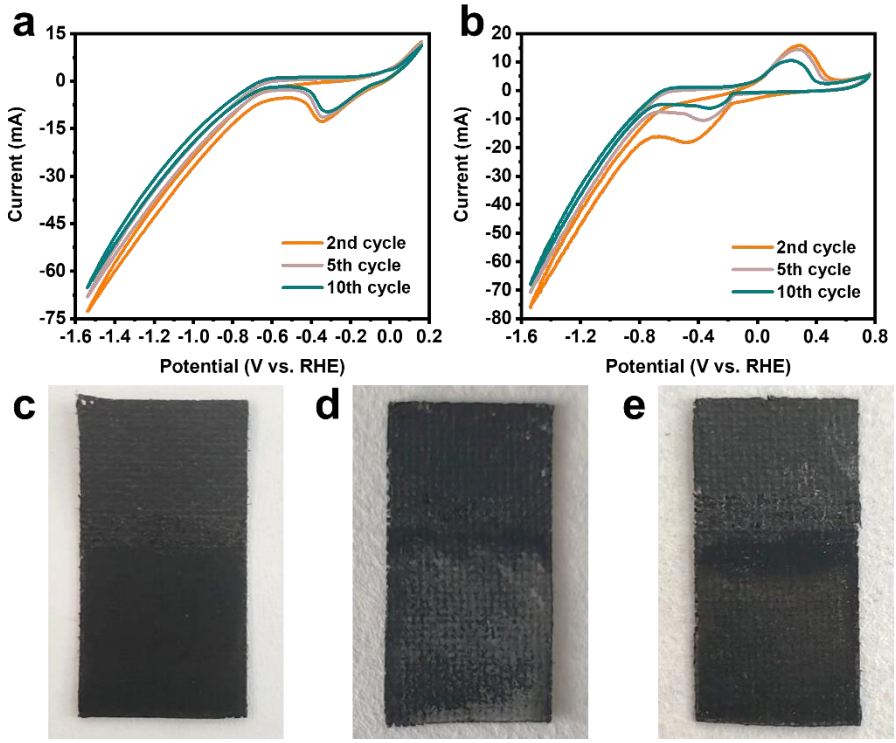

Figure S5. Cyclic voltammograms obtained at two different potential regions of (a)0.16 V~−1.54 V vs. RHE and (b) 0.76 V~−1.54 V vs. RHE at a scan rate of 50 mV/s in CO_2 saturated 0.5 M $KHCO_3$ aqueous solution; The optical photographs of (c) SnS_x/CC, (d) $SnS_{0.09}$/CC and (e) $SnS_{0.55}$/CC.

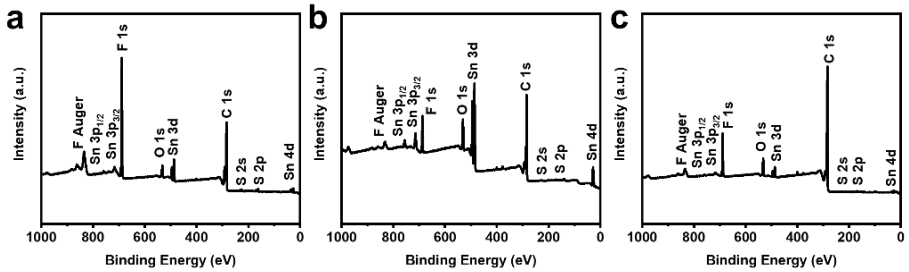

Figure S6. XPS survey spectra of (a) SnS_x/CC, (b) $SnS_{0.09}$/CC and (c) $SnS_{0.55}$/CC.

Table S1. The elemental content analysis of the XPS of SnS_x/CC, $SnS_{0.09}$/CC and $SnS_{0.55}$/CC.

Atom %	SnS_x/CC	$SnS_{0.09}$/CC	$SnS_{0.55}$/CC
C	68.74	40.95	36.76
O	28.03	47.21	58.52
F	2.23	8.94	4.22
S	0.42	0.22	0.12
Sn	0.3	2.51	0.22
Sn/S	1/1.4	1/0.09	1/0.55

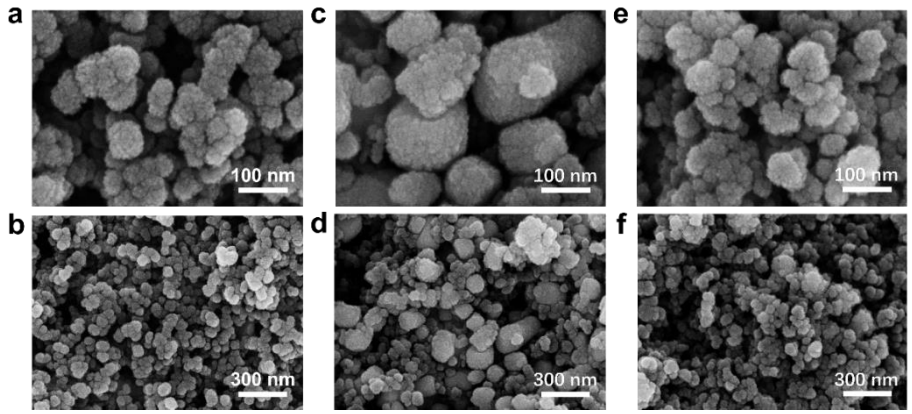

Figure S7. SEM images of (a, b) SnS_x/CC, (c, d) $SnS_{0.09}$/CC and (e, f) $SnS_{0.55}$/CC.

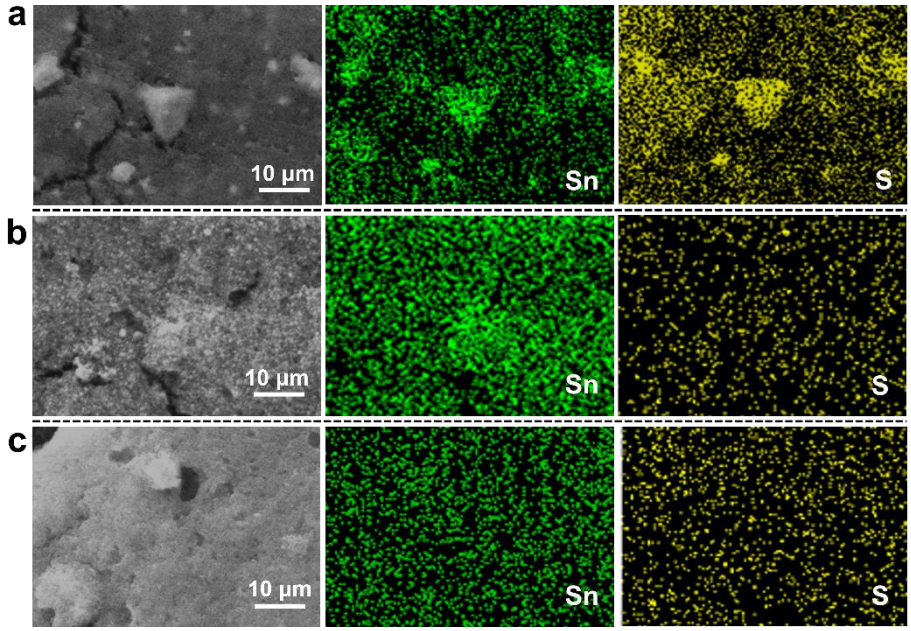

Figure S8. EDS elemental mapping of (a) SnS_x/CC, (b) $SnS_{0.09}$/CC and (c) $SnS_{0.55}$/CC.

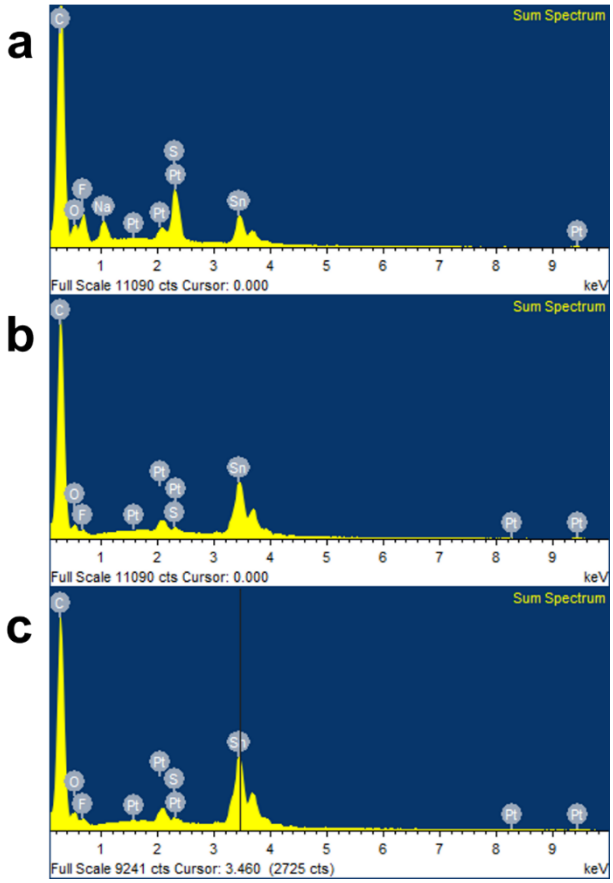

Figure S9. The EDS spectra of (a) SnS_x/CC, (b) $SnS_{0.09}$/CC and (c) $SnS_{0.55}$/CC.

Table S2. The elemental content analysis of the EDS of SnS_x/CC, $SnS_{0.09}$/CC and $SnS_{0.55}$/CC.

Atom %	SnS_x/CC	$SnS_{0.09}$/CC	$SnS_{0.55}$/CC
C	82.23	84.13	91.50
O	7.83	10.25	4.86
F	6.66	2.08	2.80
Na	0.87	--	--
S	1.43	0.27	0.22
Sn	0.85	3.00	0.47
Pt	0.14	0.27	0.16
Sn/S	1/1.68	1/0.09	1/0.47

Figure S10. Photograph of the H-cell containing 180 mL of 0.5 M $KHCO_3$ with two compartments separated by the Nafion 117 membrane.

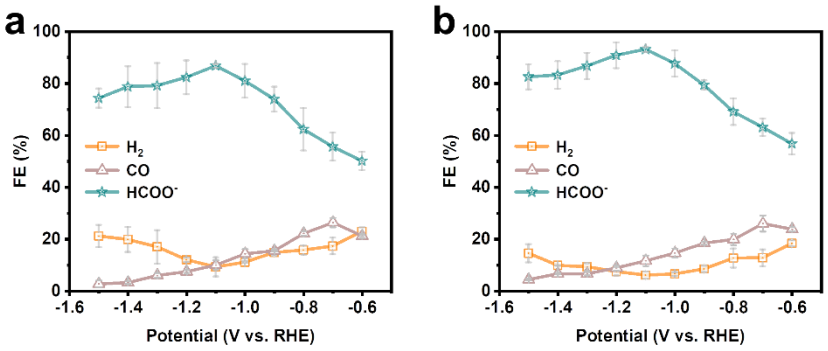

Figure S11. Potential-dependent FEs of CO, H_2 and formate over the (a) $SnS_{0.09}$/CC and (b) $SnS_{0.55}$/CC.

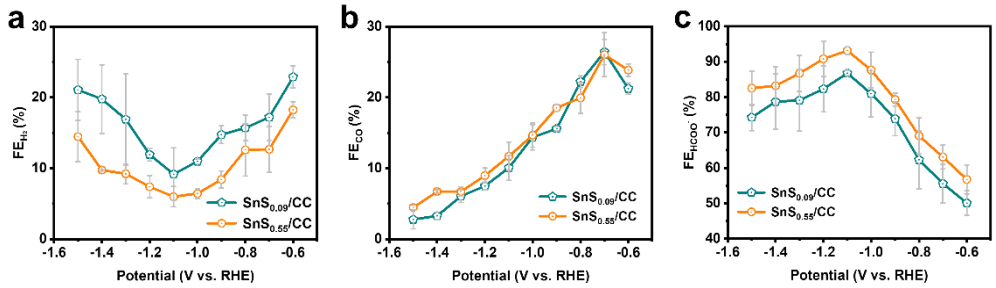

Figure S12. Potential-dependent FEs of (a) CO, (b) H_2 and (c) formate over the $SnS_{0.09}$/CC and $SnS_{0.55}$/CC.

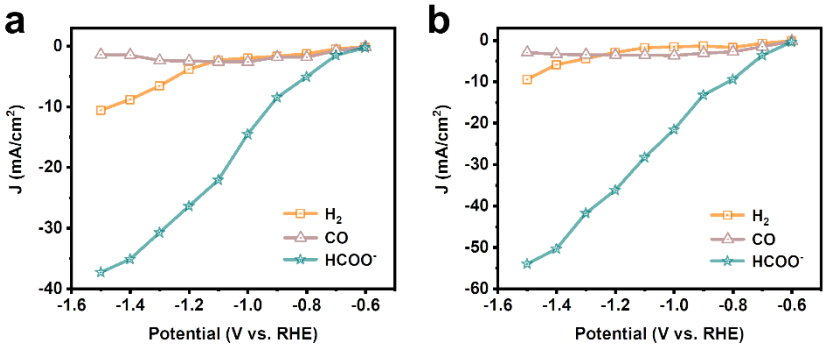

Figure S13. Partial current densities over the (a) $SnS_{0.09}$/CC and (b) $SnS_{0.55}$/CC.

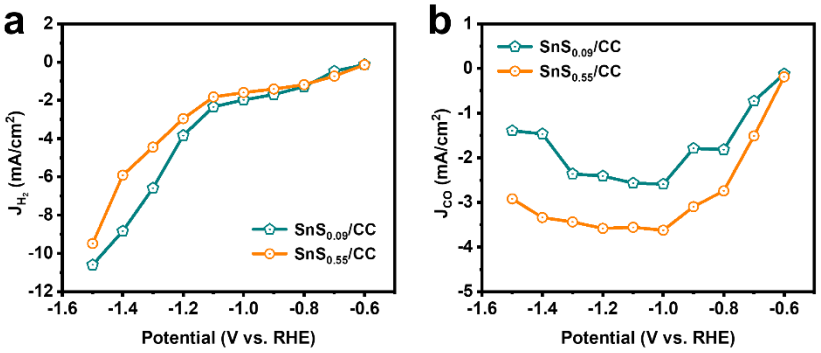

Figure S14. Partial current densities of (a) H_2 (J_{H_2}) and (b) CO (J_{CO}) over the $SnS_{0.09}$/CC and $SnS_{0.55}$/CC.

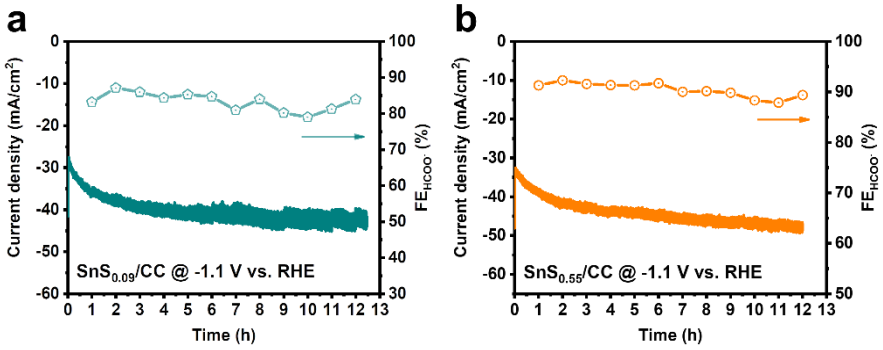

Figure S15. Stability tests of (a) $SnS_{0.09}$/CC and (b) $SnS_{0.55}$/CC at −1.1 V vs. RHE in 0.5 M $KHCO_3$ solution.

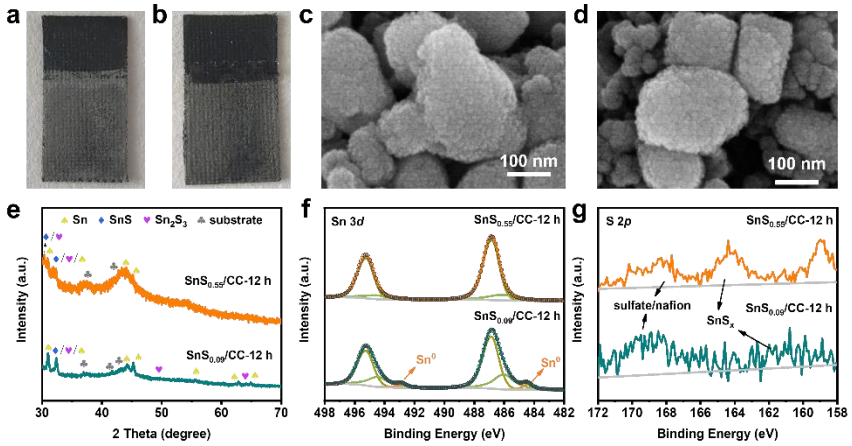

Figure S16. The optical photographs of (a) $SnS_{0.09}$/CC and (b) $SnS_{0.55}$/CC after a 12-h stability test. SEM images of (c) $SnS_{0.09}$/CC and (d) $SnS_{0.55}$/CC after a 12-h stability test. (e) XRD patterns, (f) Sn 3*d* XPS spectra and (g) S 2*p* XPS spectra of $SnS_{0.09}$/CC and $SnS_{0.55}$/CC after a 12-h stability test.

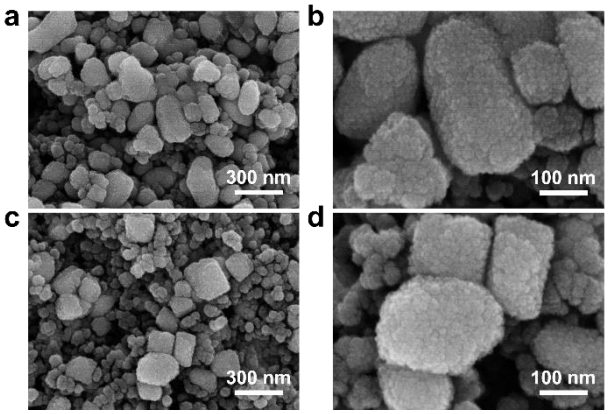

Figure S17. SEM images of (a, b) $SnS_{0.09}$/CC and (c, d) $SnS_{0.55}$/CC after a 12-h stability test.

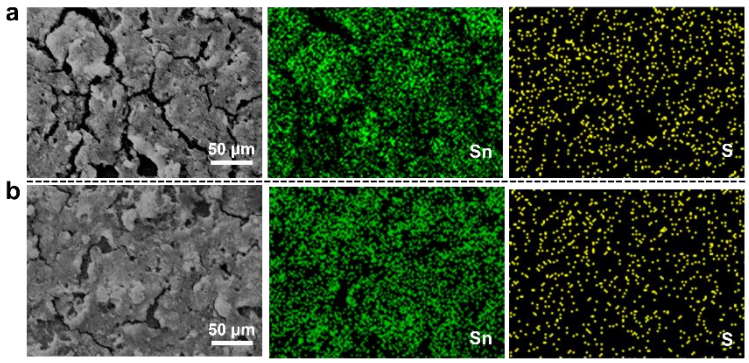

Figure S18. EDS elemental mapping of (a) $SnS_{0.09}$/CC and (b) $SnS_{0.55}$/CC after a 12-h stability test.

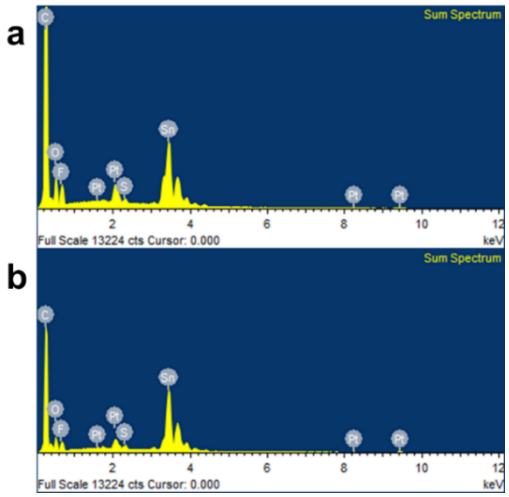

Figure S19. The EDS spectra of (a) $SnS_{0.09}$/CC and (b) $SnS_{0.55}$/CC after a12-h stability test.

Table S3. The elemental content analysis of the EDS of SnS_x/CC, $SnS_{0.09}$/CC and $SnS_{0.55}$/CC after a 12-h stability test.

Atom %	$SnS_{0.09}$/CC	$SnS_{0.55}$/CC
C	71.07	76.20
O	15.52	13.77
F	7.29	7.24
S	0.30	0.18
Sn	5.42	2.28
Pt	0.40	0.33
Sn/S	1/0.05	1/0.08

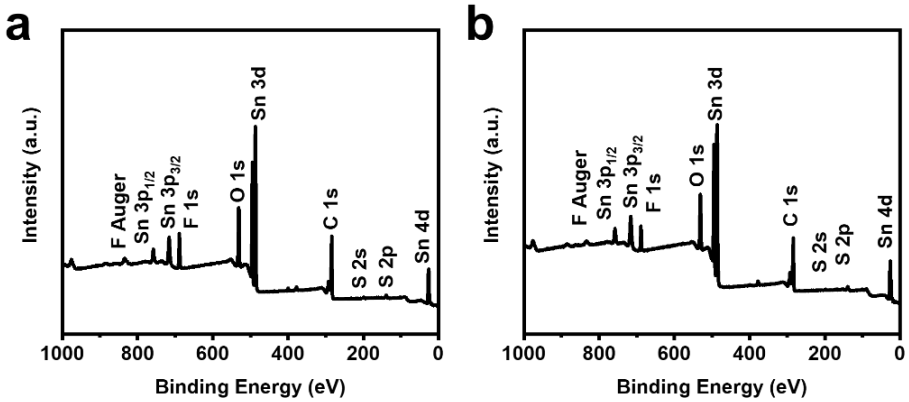

Figure S20. XPS survey spectra of (a) $SnS_{0.09}$/CC and (b) $SnS_{0.55}$/CC after a 12-h stability test.

Table S4. The elemental content analysis of the XPS of SnS_x/CC, $SnS_{0.09}$/CC and $SnS_{0.55}$/CC after a 12-h stability test.

Atom %	$SnS_{0.09}$/CC	$SnS_{0.55}$/CC
C	30.73	37.7
O	45.94	43.23
F	17.42	14.59
S	0.10	0.16
Sn	5.92	4.31
Sn/S	1/0.02	1/0.04

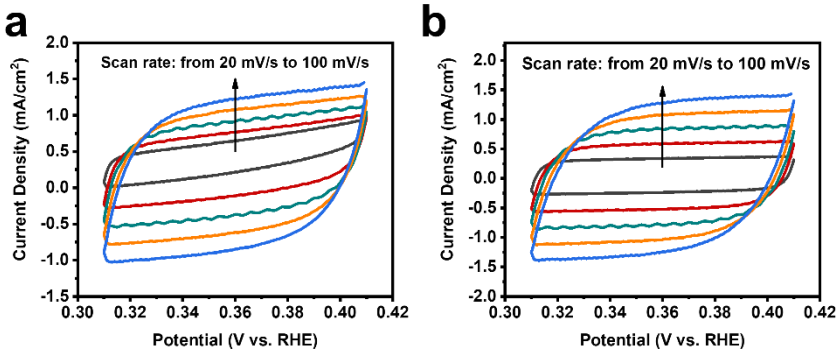

Figure S21. CV curves of the (a) $SnS_{0.09}$/CC and (b) $SnS_{0.55}$/CC with various scan rates.

Table S5 Comparisons of recently reported tin sulfide electrocatalysts for CO_2RR to formate.

Catalysts	Reaction temperature (℃)	Electrolyte	Potential (V vs. RHE)	FE($HCOO^-$)	J_{HCOO^-} (mA/cm^2)	Reference
$SnS_{0.55}$/CC	**60**	**0.5 M $KHCO_3$**	**−1.1 V**	**93.1%**	**28.4**	**This work**
$SnS_{0.09}$/CC	**60**	**0.5 M $KHCO_3$**	**−1.1 V**	**86.8%**	**22.1**	**This work**
SnS_2/rGO	180	0.5 M $NaHCO_3$	−0.76 V	84.5 %	11.8	1[1]
5%Ni-SnS_2	190	0.1 M $KHCO_3$	−0.9 V	80.0%	15.7	2[2]
$SnS_{2-x}O_x$/CC	300	0.5 M $KHCO_3$	−0.9 V	83.2 %	20.1	3[3]
H-SnS_2	160	0.1 M $KHCO_3$	−0.9 V	87.0%	24.4 (−1.0 V)	4[4]
Ag-SnS_2	210	0.5 M $KHCO_3$	−0.9 V	65.5 %	23.3 (−1.0 V)	5[5]
SnS/Aminated-C	500	0.5 M $KHCO_3$	−0.9 V	92.6 %	41.1	6[6]
SnS NSs	500	0.5 M $KHCO_3$	−1.1 V	82.1%	18.9	7[7]
SnS/Sn-NSC	800	0.5 M $KHCO_3$	−0.7 V	91.0%	5.3	8[8]
In-O-ultrathin-SnS_2	200	0.5 M $KHCO_3$	−1.2 V	88.6%	22.7	9[9]

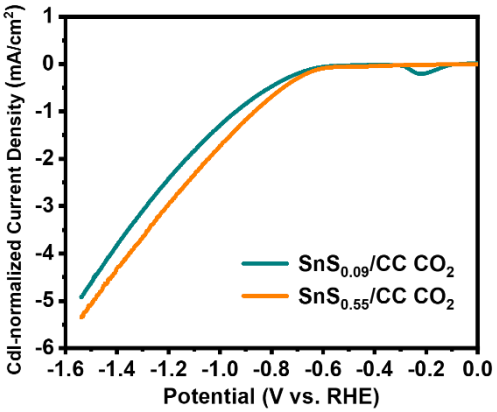

Figure S22. The Cdl-normalized current densities over the $SnS_{0.09}$/CC and $SnS_{0.55}$/CC.

References

[1] F. Li, L. Chen, M. Xue, T. Williams, Y. Zhang, D. R. MacFarlane and J. Zhang, *Nano Energy* 2017, 31, 270.

[2] A. Zhang, R. He, H. Li, Y. Chen, T. Kong, K. Li, H. Ju, J. Zhu, W. Zhu and J. Zeng, *Angew Chem. Int. Ed.* 2018, 57, 10954.

[3] T. Chen, T. Liu, T. Ding, B. Pang, L. Wang, X. Liu, X. Shen, S. Wang, D. Wu, D. Liu, L. Cao, Q. Luo, W. Zhang, W. Zhu and T. Yao, *Nano-Micro Lett.* 2021, 13, 189.

[4] A. Zhang, Y. Liang, H. Li, S. Wang, Q. Chang, K. Peng, Z. Geng and J. Zeng, *Nano Lett.* 2021, 21, 7789.

[5] R. He, X. Yuan, P. Shao, T. Duan and W. Zhu, *Small* 2019, 15, 1904882.

[6] Z. Chen, X. Zhang, M. Jiao, K. Mou, X. Zhang and L. Liu, *Adv. Energy Mater.* 2020, 10, 1903664.

[7] H. Chen, J. Chen, J. Si, Y. Hou, Q. Zheng, B. Yang, Z. Li, L. Gao, L. Lei, Z. Wen and X. Feng, *Chem. Sci.* 2020, 11, 3952.

[8] S. Zhao, Y. Qin, T. Guo, S. Li, X. Liu, M. Ou, Y. Wu and Y. Chen, *ACS Appl. Nano Mater.* 2021, 4, 2257.

[9] X. Zhang, M. Jiao, Z. Chen, X. Ma, Z. Wang, N. Wang, X. Zhang and L. Liu, *Chem. Eng. J.* 2022, 429, 132145.